J Korean Radiol Soc 2000;42:333-339

Imaging of Melorheostosis : Emphasis on MR Imaging Findings[1]

Chang Hyon Lee, M.D., Sang Kwon Lee, M.D., Jong Yeol Kim, M.D., Shin Tae Bum, M.D., Young Whan Kim, M.D., Hyo Yong Pak, M.D., Yeong Hwan Lee, M.D.[2], Kyung Hwan Byun, M.D.[3], Yong Joo Kim, M.D., Duk Sik Kang, M.D.

Purpose: To evaluate the usefulness of various radiographic imaging modalities in the diagnosis and characterization of melorheostosis.

Materials and Methods: We retrospectively evaluated the plain film (n = 8), computed tomographic (CT) imaging (n = 5) and magnetic resonance (MR) imaging (n = 5) findings of eight patients with melorheostosis diagnosed by bone biopsy (n = 4) and characteristic radiographic findings (n = 8). MR images were obtained with a 1.5-T scanner focused on the region of maximal radiographic abnormality. Pulse sequences include T1-weighted SE, T2-weighted fast SE (n = 5) and postcontrast imaging (n = 4). In order to define subtle enhancement of the lesions, subtraction MR images were obtained in one case. Imaging findings were analyzed with particular emphasis on the distribution of lesions along the sclerotome, differential radiographic findings between diaphyseal and metaepiphyseal lesions of the long bones, as seen on plain radiographs, and the density and signal characteristics of hyperostotic lesions, as seen on CT and MR images.

Results: Characteristic distribution along the sclerotome was identified in five of eight cases mainly along C6 and 7 (n = 2) and L3, 4 and 5 (n = 3) sclerotomes. In diaphyseal melorherostosis (8/8), a characteristic finding, i.e., a wax flowing down from the candle, was identified on plain radiographs. In all three patients with metaepiphyseal melorheostosis (3/8), multiple round or oval hyperostotic lesions were seen in the epiphysis and metaphysis of the long bones. On CT, the marrow cavity was partly obliterated by hyperostotic lesions in all five patients with endosteal hyperostosis. Among these, central ground glass opacity with a sclerotic rim was seen in three patients. Periosteal hyperostosis was seen in two of five cases, being visualized as irregular excrescences in the periosteal region and surrounding soft tissue. Individual hyperostosis was visualized as hypointense on T1-weighted images and as a hyperintense center with a surrounding hypointense rim on T2-weighted images (5/5). On postcontrast images, central enhancement was noted in all four cases. In one of these, in which the degree of central enhancement was subtle, subtraction images (postcontrast SE- precontrast SE) also revealed a central signal increment. Central enhancement corresponded to the hyperintense center seen on T2-weighted images (4/4) and the ground-glass opacity seen on CT (2/2).

Conclusion: Radiographic imaging plays a crucial role in the diagnosis of melorheostosis. The future role of gadolinium-enhanced MR imaging in the characterization of the lesion may be important though further evaluation and pathologic correlation is required.

Index words : Bones, osteochondrodysplasia
Bones, radiography
Bones, CT
Bones, MR

[1]Department of Diagnostic Radiology, College of Medicine, Kyungpook National University
[2]Department of Diagnostic Radiology, College of Medicine, Catholic University of Taegu-Hyosung
[3]Department of Diagnostic Radiology, Kumi CHA General Hospital, College of Medicine, Pochon CHA University
Received April 15, 1998 ; Accepted August 25, 1999
Address reprint requests to : Sang Kwon Lee, M.D., Department of Diagnostic Radiology, School of Medicine, Kyungpook National University Hospital #52 Sam Duk Dong 2 ga Taegu, 700-412, Korea Tel. 82-53-420-5390 Fax. 82-53-422-2677 E-mail. sangklee@kyungpook.ac.kr

Melorheostosis is a rare non-inheritable disorder characterized by a flowing hyperostosis of the cortex affecting a single limb and first described by Leri and Joanny in 1922 (1). Diagnosis has been based on characteristic plain radiographic findings; to our knowledge, MR imaging findings have been reported in only two cases and contrast-enhanced MR imaging findings in only one (2, 3).

We describe the plain film, CT and MR imaging findings of melorheostosis, having evaluated the usefulness of radiographic imaging in the diagnosis and characterization of melorheostosis with particular emphasis on contrast-enhanced MR imaging findings.

Materials and Methods

Between 1987 and 1998, eight patients (six males and two females, aged 3-55 [mean, 38.3] years) were found to be suffering from melorheostosis. Diagnosis was on the basis of characteristic radiographic findings (n = 8) and the histopathologic findings of excisional bone biopsy (n = 4).

CT (n = 5) was performed with a HiSpeed Advantage scanner (GE Medical Systems, Milwaukee, U.S.A.) using the following parameters: 5-mm slice thickness, 10-mm interslice gap, 120 kVp, 280 mA, 10-mm collimation, a helical pitch of 1:1, and 25-cm field of view.

For MR imaging (n = 5), a 1.5-T unit (Signa, GE Medical Systems, Milwaukee, U.S.A.) was used. Depending on the location of the lesions, a phased-array extremity coil was sometimes employed. Imaging sequences included spin-echo (SE) and fast spin-echo (FSE) techniques, with the following acquisition parameters: 400-600/10-12 (repetition time msec/echo time msec) for T1-weighted SE images; 2,500-3,500/96-108 (repetition time msec/effective echo time msec) with an echo train length (ETL) of eight for T2-weighted FSE images, and 350-600/10-12 (repetition time msec/echo time msec) for gadolinium-enhanced T1-weighted images. The fat-suppression technique based on frequency-selective excitation was used in T2-weighted FSE and gadolinium-enhanced T1-weighted SE imaging. For both T1- and T2-weighted images, slice thickness of 3.0-7.0 mm with a 0-2.5 mm interslice gap, number of excitation (NEX) of two to four and matrix number of 256×192 were used. Field of view (FOV) was 180 to 340 mm, depending on body size and section planes. Axial and coronal or sagittal images were obtained for each pulse sequence; contrast-enhanced T1-weighted images were obtained 20 seconds after intravenous injection of gadopentetate dimeglumine at a dose of 0.1 mmol/kg of body weight. In order to define lesion enhancement, subtraction MR images (postcontrast SE - precontrast SE) on Advantage Windows workstation (GE Medical systems, Milwaukee, U.S.A.) was used. CT and MR imaging focused on the regions of maximal abnormality. Plain radiographs were available for all patients.

Imaging findings were analyzed with particular emphasis on the distribution of lesions along the sclerotome, as seen on plain films, and the density and signal characteristics of hyperostotic lesions, as seen on CT and MR images.

Results

Plain Radiographic Findings

In all eight patients with diaphyseal melorheostosis, a characteristic finding, i.e., wax flowing down the side of a candle, was identified on plain radiographs (Fig. 1). In all three cases of metaepiphyseal melorheostosis, multiple round or oval hyperostostic lesions were seen in the epiphysis and metaphysis of the long bones. In one case, combined osteopathia striata was identified in the iliopubic bone.

There were six cases of endosteal hyperostosis, in which the lesion does not extend through the periosteum, and two of the periosteal type, in which bony excrescences are seen along the periosteum. A 50-year-old male patient with extensive periosteal hyperostosis underwent surgery for progressive limb deformity.

In five of five cases, scintigraphy revealed increased uptake in the involved bones. Clinical and imaging data are summarized in the accompanying table.

CT Findings

All lesions in patients who underwent CT showed cortical thickening. In one case, abnormal dense cortical thickening scalloping normal cortex was seen. The lesions partially obliterated the marrow cavity, especially in endosteal-type cases. Central ground-glass opacity with a surrounding sclerotic rim was identified on CT in three of five patients (Fig. 1F). Extensive cauliflower-like bony excrescences are noted in one periosteal type.

MR Findings

All five lesions for which MR images were obtained showed low signal intensity on T1-weighted SE images, and central high signal intensity with a low signal inten-

Fig. 1. Images in a three-year-old female with involvement of the right lower extremity.
A. Plain radiograph shows patchy linear hyperostosis in the right pubis (black arrow) and endosteal hyperostosis in the medial side of right femur (white arrow).
B. The diaphysis of the right tibia reveals characteristic wavy hyperostosis flowing down the side.
C. Axial T1-weighted SE image (550/15) of the right tibia shows endosteal hyperostosis of low signal intensity.
D. Axial fat-suppressed T2-weighted FSE image (3,700/100) demonstrates the central high signal intensity (arrow) with surrounding rim of low signal intensity.
E. Postcontrast axial T1-weighted SE image (350/15) with fat suppression reveals central enhancement (arrow) of the lesion.
F. CT shows the central ground-glass opacity with sclerotic rim (arrow) at the comparable site of the MR images.
G. Postcontrast sagittal T1-weighted SE image (550/14) with fat suppression of the right foot also demonstrates central enhancement (arrow) of the round or oval lesions in the talus and medial cuneiform.
H. Photomicrograph of the abnormal cortex reveals irregularly thickened tabeculae and some fibrovascular tissues (Hematoxylin-eosin stain; original magnification, ×100)

sity rim on T2-weighted FSE images (Fig. 1,2). On postcontrast MR images, central enhancement with a low signal intensity peripheral rim was identified in two children and two adults. Signal increment was noted in the center of the lesions on the subtraction images obtained in the case of a 45-year-old male patient (Fig. 2E). In two children, central ground-glass opacity on CT images coincided with central enhancement on postcontrast MR images (Fig. 1E,F).

Pathologic Findings

The microphotographs obtained by excisional bone biopsy revealed irregularly thickened trabecular bones and some fibrovascular tissues (Fig. 1H). Osteoclastic or osteoblastic activity was not seen.

Discussion

Melorheostosis is a rare benign sclerosing bony dysplasia characterized by linear hyperostosis of cortical bone and joint abnormalities, and affects children and adults. Because diagnosis is based on the presence of characteristic radiographic features rather than the histopathology of the lesions, radiographic imaging plays an important role in the diagnosis of this condition (4).

The etiology of melorheostosis is not known. According to Zimmer (5), the pattern of involvement indicates that it arises from maldevelopment of the limb bud caused by metameric disturbance. Campbell (6) believes that the disorder affects not only bone but also many tissues of mesodermal origin and that the marked soft tissue changes found at birth tend to support Zimmer's concept. There is, however, no evidence that melorheostosis is a genetic disorder (7). Although most investigators believe it is congenital, symptoms do not manifest until late childhood or early adolescence (4).

Melorheostosis usually involves a single limb particularly the lower extremity, though in rare instances, more than one limb is affected. The pelvis, skull, spine, and facial bone may also be involved (6, 8-10). Murray and McCredie (11) have suggested that the skeletal lesions may represent the late result of a segmental sensory nerve lesion. The typical distribution of hyperostosis corresponds to a single sclerotome (a zone supplied by an individual spinal sensory nerve), or part of one; the skeletal lesions seen in all our patients corresponded to sclerotomes or a part of one. Two children showed the same distribution of lesions.

Hyperostosis tends to progress through childhood and the disease exhibits a slow, chronic course with periods of exacerbation and arrest (6). Most evidence of progression of the condition is based on the increased hyperostosis seen on radiographs obtained at periodic intervals, and on the findings of several biopsies. It can also progress in adults, manifesting as an aggravation of symptoms, soft-tissue abnormalities, and bone involvement, although in adults the process is not as active or rapidly progressive as in children (6). We observed the progression of this

Table. Clinical and Imaging Data in Patients with Melorheostosis

No/Age/Sex	Sx	Location	CT findings	MR findings			
				T1WI	T2WI	Enhancement	Subtraction
1/3/F	Varus deformity	Right pubis, femur, tibia, talus, cuneiform, phalanges	Cortical thickening with ground-glass opacity	Low SI	Central high SI with low SI rim	Central enhancement	
2/9/M	Bowing	Right pubis, femur, tibia, talus, cuneiform, phalanges	Cortical thickening	Low SI	Central high SI with low SI rim	Central enhancement	
3/34/M	Incidental	Right ulnar	Cortical thickening with ground-glass opacity				
4/40/M	Incidental	Left scapula, rib, clavicle, humerus, radius, carpal bones, phalanges	Cortical thickening with ground-glass opacity				
5/45/M	Joint pain	Right tibia		Low SI	Central high SI with low SI rim	Subtle central enhancement	Central signal increment
6/50/M	Deformity	Right scapula, calvicle, humerus, radius, ulnar, carpal bones, phalanges	Cortical thickening with bony excrescences				
7/55/F	Joint pain	Right Phalanges		Low SI	Central high SI with low SI rim	Central enhancement	
*8/35/M	Incidental	Right femur, patella, tibia, phalanges		Low SI	Central high SI with low SI rim		

T1WI = T1-weighted images, T2WI = T2-weighted images, SI = signal intensity
*This case was combined with osteopathia striata

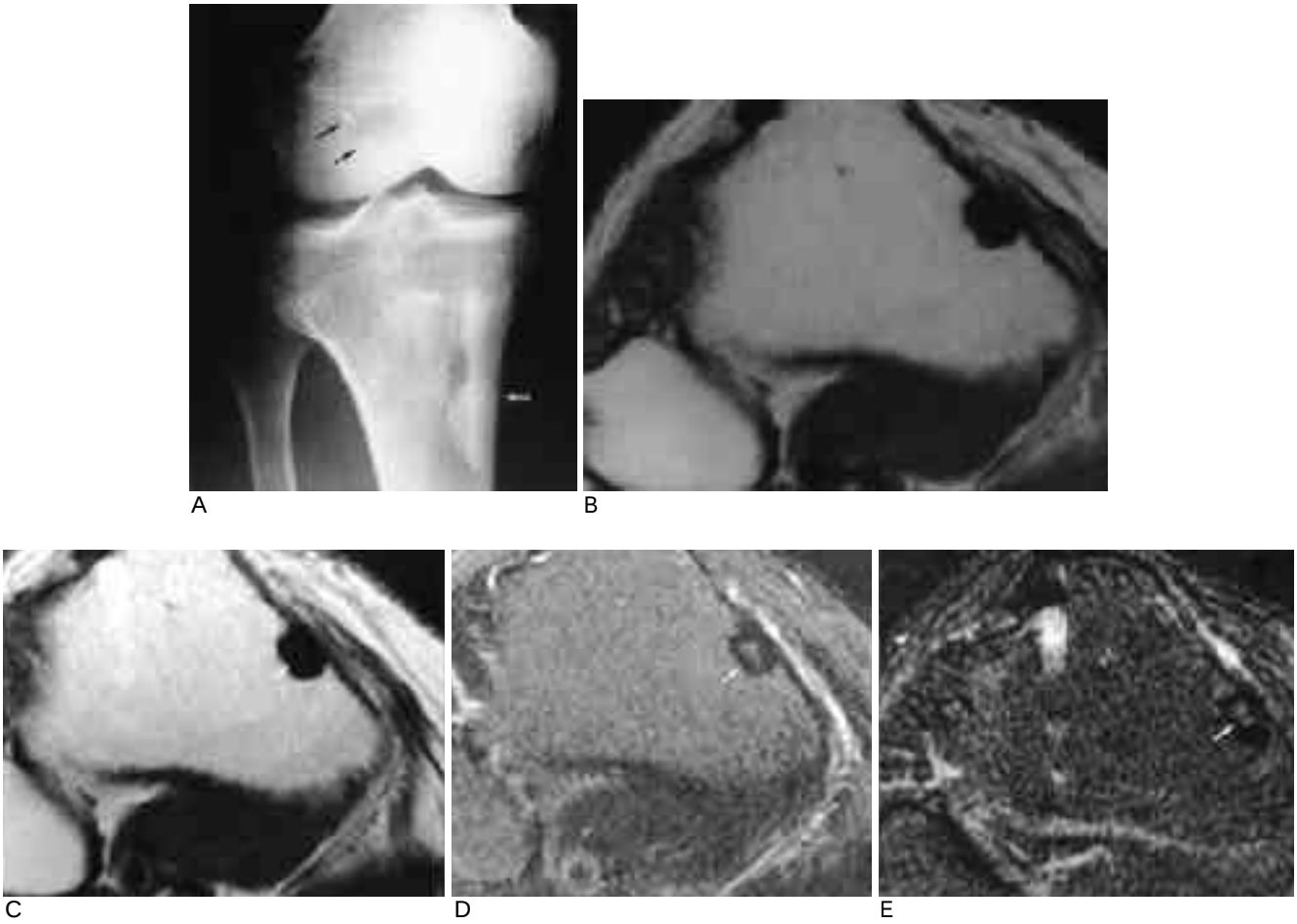

Fig. 2. Images in a 45-year-old male with right knee joint pain.
A. Plain radiograph of the right knee reveals ovoid hyperdense lesions in the distal epiphysis (black arrow) of the femur and hyperostosis along the medial side of the diaphysis (white arrow) of tibia.
B. Axial T1-weighted SE image (600/12) of the right proximal tibia shows ovoid nodular hyperostosis of low signal intensity.
C, D. The central portion of the lesion is slightly enhanced (arrow) on the postcontrast axial T1-weighted SE image (600/12) and reveals high signal intensity (arrow) on the axial T2-weighted FSE image (3000/108).
E. The subtraction image (postcontrast T1-weighted SE image minus precontrast T1-weighted SE image) demonstrates central signal increment (arrow).

disorder in a 50-year-old male who underwent surgery for limb deformity.

The features of the disease in children are slightly different from those in adults. Clinically, pain occurs infrequently in children and is not intense; radiographically, the endosteal type is frequently reported in childhood though it can also be seen in adults (12).

Melorheostosis has been reported in association with other disorders including linear scleroderma, osteopoikilosis, osteopathia striata, neurofibromatosis, tuberous sclerosis and hemangioma or other vascular lesions (13-19). The entity was described by Walker in 1964 as mixed sclerosing bone dystrophy (20). In one of our cases, melorheostosis was combined with osteopathia striata in the pubic bone, but linear scleroderma or other skin change was not seen in our patient.

The histologic features of melorheostosis have been reported by a number of authors (4, 11, 17). Microscopic examination of cortical specimens reveals nonspecific, hyperostotic, periosteal bone exhibiting thickened trabeculae and some fibrovascular tissues in the marrow spaces. The immature bone consists largely of primary haversian systems, particularly on the periosteal surface, that are almost obliterated by the deposition of sclerotic, thickened, and somewhat irregular lamellae. Osteoclastic or osteoblastic activity can be noted but is never prominent.

Roentgenographic findings have on occasion been used for diagnosis. Irregular, dense, eccentric hyperostosis affecting both the cortex and adjacent medullary canal of a single bone, or one side of the limb, like melted wax dripping down the side of a candle, is highly characteristic. In the epiphysis of long bones, more dis-

crete round foci may resemble the findings of osteopoikilosis, whereas in flat bones such as those in the pelvis, or the scapula, radiating or localized sclerotic patches are seen (21).

CT findings are described as simple cortical thickening and osseous excrescence on the external and/or internal cortical surfaces (21). On occasion, these changes partly or completely obliterate the marrow cavity, particularly in the endosteal type. In two children and two adults, we found that density was less than that of normal cortex in the endosteal area occupying the marrow cavity just beneath the thickened cortex. This ground-glass opacity was centrally located and surrounded by a sclerotic rim. We speculated that the difference in density between the abnormal dense cortex and the central ground glass opacity in the diaphysis was either due to the varying amounts of intramembranous ossification found along the periosteum, or the process of change from a less mature lesion to mature dense cortex. Greenspan (4) also believes that radiographic findings appear to reflect developmental errors at the sites of intramembranous and endochondral bone formation, predominantly the former.

To our knowledge, MR imaging findings of melorheostosis have been published in only two cases (2, 3), only one of which included the findings of postcontrast MR imaging (3). They found that a metaphyseal lesion of the distal femur showed low signal intensity on both T1- and T2-weighted images, with peripheral rim enhancement, speculating that the lesion was one which was less mature and the enhancing rim was consistent with the vascular fibrous reaction about centrally located aberrant bony proliferation (3).

Empirically, we had expected that on MR images, cortical hyperostosis might show low signal intensity on all pulse sequences, but on T2-weighted images, all the lesions in fact showed central high signal intensity, with a low signal intensity rim. Unexpectedly we experienced central enhancement on postcontrast images in four patients for whom contrast-enhanced MR images were available. In one case, in which subtle central enhancement was observed, subtraction imaging also revealed central signal increment.

In our study, the central portion of the lesions showing contrast enhancement was - in two cases in which both CT and MR findings were available - comparable to the area of central high signal intensity seen on T2-weighted images and the ground-glass opacity seen on CT. We considered that this central enhancement was caused by fibrovascular reaction about the thickened rim of trabecular bones. Interestingly, all the central ground-glass opacity seen on CT, and the central enhancement seen on postcontrast MR images, was found only in children and symptomatic young adults. In view of these clinical findings, central enhancement seems to be related to disease activity.

In conclusion, radiographic imaging plays a crucial role in the diagnosis of melorheostosis. The central ground-glass opacity seen on CT and central enhancement seen on postcontrast MR images are probably related to lesion activity, though further study is required.

References

1. Leri A, Joany L. Une affection non decrite des os: Hyperostose《en coulee》sur toute la longueur d 'un membre ou《melorheostose》. *Bull Mem Soc Med Hosp Paris* 1922;46:1141-1145
2. Isaac P, Resnick D. MR appearance of axial melorheostosis. *Skeletal Radiol* 1993;22:47-48
3. Yu JS, Resnick D, Vaughan LM, Haghishi P, Hughes T. Melorheostosis with an ossified soft tissue mass: MR features. *Skeletal Radiol* 1995;24:367-370
4. Greenspan A. Sclerosing bone dysplasias: a target-site approach. *Skeletal Radiol* 1991;20:561-583
5. Zimmer P. Uber einen Fall einer eigenartigen seltenen Knockenerkrankung:osteopathia hyperostotica-melorheostoise. *Beitr Klin Chir* 1927;140:75-85
6. Campbell CJ, Papademetriou T, Bonfiglio M. Melorheostosis: a report of the clinical, roentgenographic, and pathological findings in fourteen cases. *J Bone Joint Surg [Am]* 1968;50:1281-1304
7. Fairbank HAT. Osteopathia striata. *J Bone Joint Surg [Br]* 1950;32:117-125
8. Williams JW, Monaghan D, Barrington NA. Cranio-facial melorheostosis: case report and review of the literature. *Br J Radiol* 1991;64:60-62
9. Raby N, Vivian G. Case report 478: melorheostosis of the axial skeleton with associated intrathecal lipoma. *Skeletal Radiol* 1988;17:216-219
10. Garver P, Resnick D, Haghighi P, Guerra J. Melorheostosis of the axial skeleton with associated fibrolipomatous lesions. *Skeletal Radiol* 1982;9:41-44
11. Murray RO, Mccredie J. Melorheostosis and the sclerotome: a radiological correlation. *Skeletal Radiol* 1979;4:57-71
12. Younge D, Drummond DS, Herring J, Cruess RL. Melorheostosis in children. *J Bone Joint Surg [Br]* 1979;61-B:415-418
13. Abrahamson MN. Disseminated asymptomatic osteosclerosis with features resembling melorheostosis, osteopoikilosis, and osteopathia striata. *J Bone Joint Surg [Am]* 1968;50:991-996
14. Buchmann J. Osteopoikilie und melorheostose. *Beitr Orthop Traumatol* 1968;15:641-642
15. Wellmitz G. Ein Beitrag zum Krankheitsbild der Melorheostose und Osteopoikilie. *Beitr orthop Traumatol* 1972;19:117-126
16. Mccarroll HR. Clinical manifestations of congenital neurofibromatosis. *J Bone Joint Surg [Am]* 1950;32:601-617
17. Hall GS. A contribution to the study of melorheostosis:unusual bone changes associated with tuberous sclerosis. *Q J Med* 1943;12:77-100

18. Patrick JH. Melorheostosis associated with arteriovenous aneurysm of the left arm and trunk: report of a case with long follow up. *J Bone Joint Surg [Br]* 1969;51:126-134
19. Kessler HB, Recht MP, Dalinka MK. Vascular anomalies in association with osteodystrophies-a spectrum. *Skeletal Radiol* 1983; 10:95-101
20. Walker GF. Mixed sclerosing bone dystrophies: two case reports. *J Bone Joint Surg [Br]* 1964;46:546-552
21. Resnick D. *Diagnosis of bone and joint disorder. Melorheostosis*. Philadelphia :Saunders, 1995:4410-4416

대한방사선의학회지 2000;42:333-339

유선상과골증의 영상소견 : 자기공명영상 소견을 중심으로[1]

[1]경북대학교 의과대학 진단방사선과학교실
[2]대구효성가톨릭대학교 의과대학 진단방사선과학교실
[3]포천중문의과대학 구미차병원 진단방사선과학교실

이창현 · 이상권 · 김종열 · 신태범 · 김영환 · 박효용 · 이영환[2] · 변경환[3] · 김용주 · 강덕식

목적 : 유선상과골증의 특징적인 영상소견을 알아보고 조영증강 자기공명영상의 유용성에 대하여 알아보고자 하였다.

대상과 방법 : 골 생검과(n=4) 특징적인 방사선학적 소견으로(n=8) 진단된 8예의 유선상과골증의 단순촬영(n=8), 전산화 단층촬영(n=5) 및 자기공명영상(n=5) 소견을 후향적으로 분석하였다. 자기공명영상은 1.5-T 초전도영상장치를 이용하였고, 방사선학적 소견이 가장 심한 부위를 중심으로 평가하였다. 스핀에코기법을 이용한 T1강조영상, 급속 스핀에코기법을 이용한 T2강조영상을 얻었으며 4예(4/5)에서 조영증강후 영상을 얻었다. 1예에서는 미약한 조영증강의 유무를 확인하기 위하여 감산영상을 얻었다. 영상 소견은 sclerotome에 따른 병변의 분포 간 병변과 골간단 및 골단 병변의 영상소견의 차이, CT와 MR imaging에서의 과골화 병변의 밀도 및 신호강도의 특징을 중심으로 분석하였다.

결과 : Sclerotome에 따른 특징적인 분포양상은 5예(5/8)에서 관찰되었으며, C6, 7이 2예(2/5), L3, 4, 5가 3예 (3/8)였다. 단순 촬영에서 골간의 병변은 촛물이 초의 한쪽 벽을 따라 흘러 내려오는 양상의 특징적인 소견을 (8/8) 보였으며, 골단 또는 골간단에서는 다수의 원형 또는 난형의 병변으로 (3/8) 관찰되었다. Endosteal hyperostosis는 CT를 시행한 5예(5/5) 전부에서 골수강을 차지하는 고밀도의 병변으로 보였으며, 이들 중 3예(3/5)에서 중심부 간유리음영과 주변부 골경화성 변연이 관찰되었다. Periosteal hyperostosis는 2예(2/5)에서 관찰되었고, 골주위와 주위 연부조직을 침범하는 고음영의 증식성 골병변으로 보였다. 각각의 hyperostosis는 T1강조영상에서는 중심부와 주변부의 구별 없이 저신호강도로 관찰되었고. T2강조영상에서는 고신호강도의 중심부와 주변부의 저신호강도의 변연으로 관찰되었다 (5/5). 조영증강후 영상을 얻었던 4예 전부에서 중심부 조영증강이 관찰되었으며 (4/4), 조영증강이 미약하였던 1예(1/4) 에서는 감산영상에서 조영증강을 확인할 수 있었다. 조영증강된 중심부는 T2강조영상에서의 고신호강도와 일치하였고 (4/4), CT에서의 중심부 간유리음영과 (2/2) 일치하였다.

결론 : 방사선학적 영상은 유선상과골증의 진단에 중요하며, 조영증강후 자기공명영상은 병변의 특성화에 있어서 중요한 역할을 할 것으로 기대된다.

《 저작권에 관한 동의서 》

_____

라는 제목의 논문이 대한방사선의학회지에 출간될 경우 그 저작권을 대한방사선의학회에 이전한다.

저자는 저작권이외의 모든 권한 즉, 특허신청이나 향후 논문을 작성하는데 있어서 본논문의 일부 혹은 전부를 사용하는 등의 권한을 소유한다. 저자는 대한방사선의학회지로부터 서면허가를 받으면 타논문에 본 논문의 자료를 사용할 수 있으며 이 경우 자료가 발표된 원논문을 밝힌다. 본논문의 모든 저자는 본논문에 실제적이고 지적인 공헌을 하였으며 논문의 내용에 대하여 공적인 책임을 공유한다.

본논문은 과거에 출판된 적이 없으며 현재 타학술지에 제출되었거나 제출할 계획이 없다.

제 1저자/ 년 월 일	제 2저자	제 3저자
제 4저자	제 5저자	제 6저자

[분 야: _____]

본 동의서는 원고에 기술된 순서대로 전 저자의 서명이 있어야 함.

대한방사선의학회 원고 최종 점검표

- □ **원고 1부, 사진 1부를 동봉한다.**
- □ **행간 여백 1행(double space)에 21×30cm (A4)용지에 작성한다.**
- □ **원고배열은 한글과 영문으로 기재된 표지, 내표지, 초록(한글과 영문), 서론, 대상과 방법, 결과, 고찰, 참고문헌, 표, 사진설명의 순으로 한다.**
- □ **초록은 목적, 대상과 방법, 결과, 결론으로 나누어 기술한다.**
- □ **영문초록 하단에 색인단어 (Index Words)를 기입한다.**
- □ **저작권에 관한 동의서에 전 저자가 서명한다.**
- □ **투고규정내의 저자 점검사항을 점검하였다.**